Presentation for ISINN31
May 26—May 30 Dongguan, China

Progress of Shielding Integral Experiments at China Institute of Atomic Energy

YangBo-Nie, ShiYu-Zhang, YanYan-Ding, Qi-Zhao, KuoZhi-Xu, XinYi-Pan

ShiYu-Zhang

Key Laboratory of Nuclear Data
China Nuclear Data Center(CNDC)
China Institute of Atomic Energy(CIAE)
Lanzhou Univeristy(LZU)
Beijing 102413, P.R.China
E-Mail: zsy20821@126.com

Content

The Use of Nuclear Data

Data Measurement
Nuclear structure data,
Nuclear reaction data,
Benchmark experiment
……

Model theory
Nuclear reaction、
Nuclear structure……

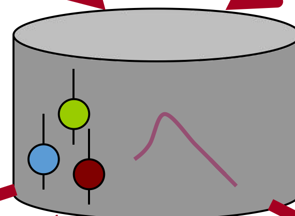

Nuclear data libraries
-Experimental nuclear database
-Evaluated nuclear database
-Dedicated nuclear database

Scientific research:
Nuclear physics,
Nuclear reactor physics ……

Nuclear technology application:
Nuclear medicine,
Nuclear detection technology……

Nuclear energy development:
Nuclear power,
Nuclear fuel cycle……

National defense construction:
Design, Test, Maintenance and storage, Nuclear power……

Public education:
Science education,
Professional Education……

➢**The precision and reliability of nuclear data are directly related to the quality of nuclear engineering products and the application of nuclear technology**

Nuclear Data Production

Basic study of nuclear physics

Reaction and Structure theory

Fundamental experimental data

Modeling codes predictions

Evaluations

Data Processing

Application libraries

Transport simulation of integral experiments

Feedback

Integral experimental data

Check the quality of nuclear data

Application (Users)

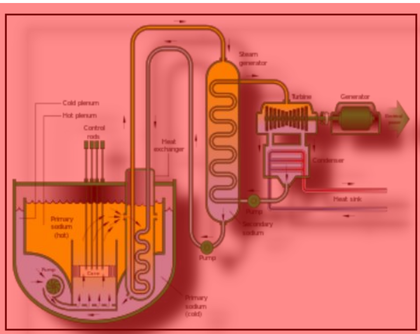

Engineering design

Nuclear weapon design

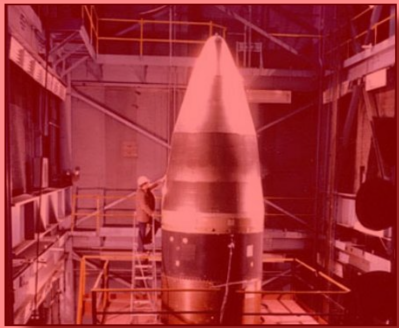

Integral experiment is an essential part of evaluating nuclear data before it is provided to users.

CIAE Integral Experiment Arrangement

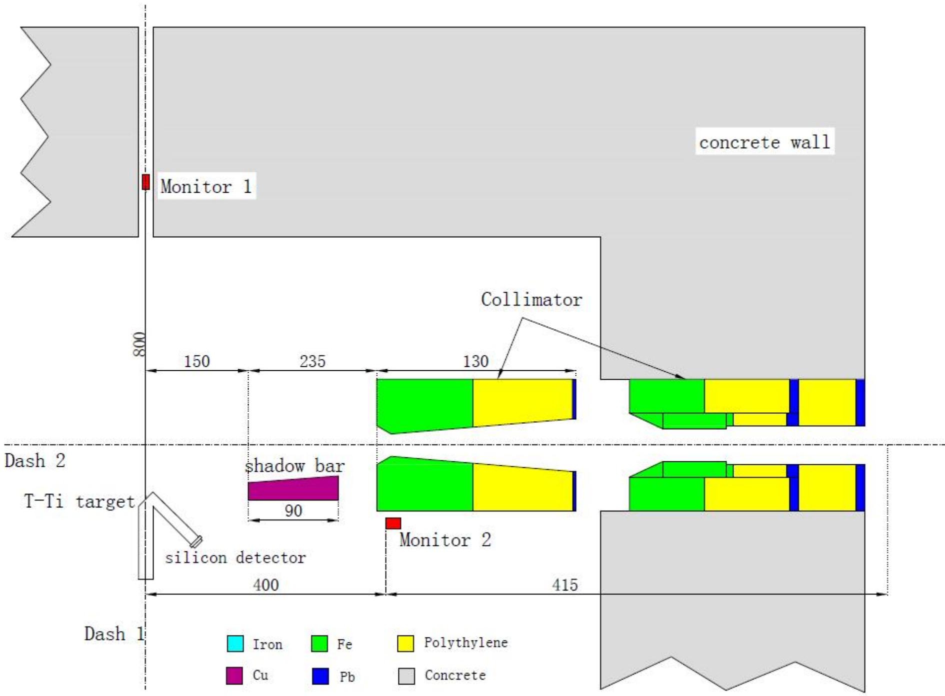

Measure TOF spectra of leakage neutrons at >90°.
Effect/background ratio reaches top international level.

Table1. The integral experiments have been performed at CIAE

Sample	Size (cm)	Thickness (cm)	Angle (°)
^{238}U	10×10	5	45,135
Be	10×10	5,11	60,120
^{nat}Ga	Φ13	3.2,6.4	60,120
^{nat}W	10×10	3.5,7	60,120
W	10×10	5	60
C	Φ13	20	60,120
^{238}U	10×10	2,5,11	60,120
SiC	Φ13	20	60,120
Pb	Φ13	5	60
Pb-Bi	Φ13	5	60
ThO_2	Φ13	10.8	60,120
H_2	Φ13	10.8	60
Polyethene	Φ13	6	60
	10×10	5,6	45,60

Current Focus of Integral Experiments

Current integral experiments focus on precise measurements at multiple angles and thicknesses for key nuclides.

Experiments are conducted with 3 thicknesses and 6 detection angles.

The platform upgrade to enable higher-precision TOF measurements.

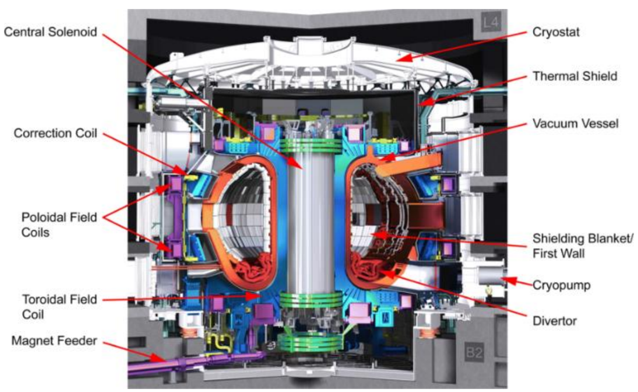

Beryllium

Widely used in **fusion reactors**
Key material for neutron multiplier and shielding

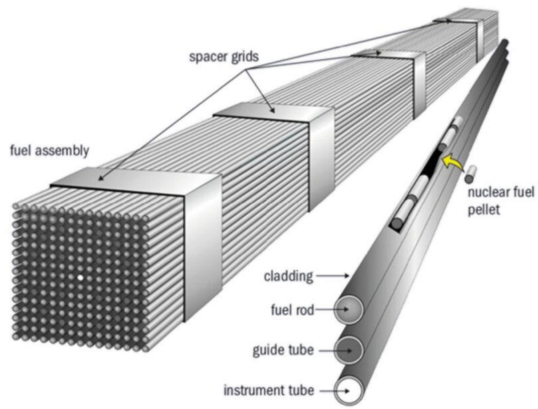

Zirconium

Common in **reactor structural components**
Low absorption, good for neutron economy

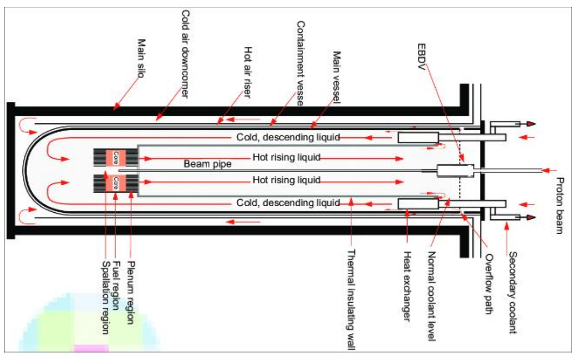

Bismuth

Component of **Pb-Bi eutectic coolant**
Applied in **lead-cooled fast reactors (LFRs)** and **ADS**

Experimental Platform Upgrades for High-Precision TOF Measurements

① Digital Electronics & Full Waveform Recording

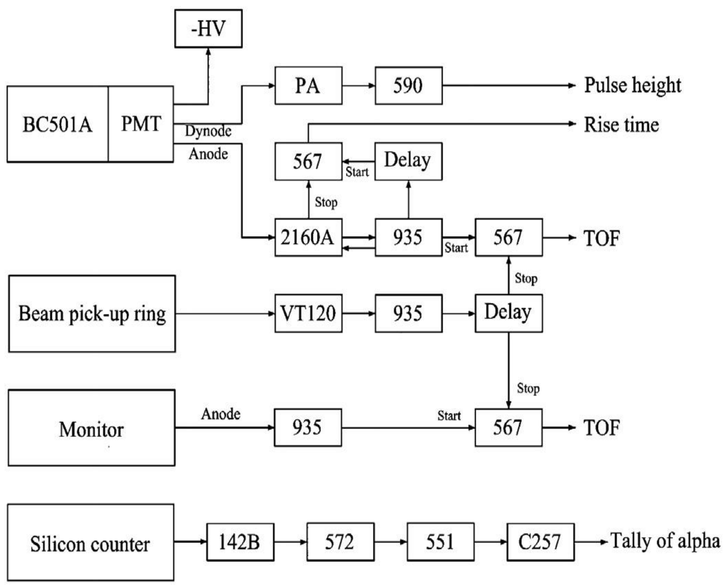

Parameter	Value
Number of Channels	16
Sampling Rate	500 MS/s
Resolution	12 bit
Max Acquisition Time per Waveform	20 μs
Data Transfer Rate	10^9 MS/s

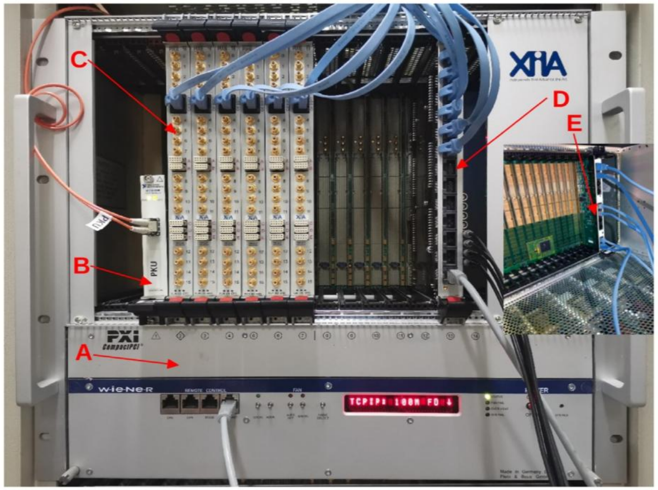

①Replaced traditional analog electronics with digitized acquisition system;
②Enables full waveform recording for advanced data processing and analysis.

② Accurate Pulse Time Distribution Shape Monitoring with Liquid Scintillator

① Liquid scintillator monitor + deconvolution algorithm;

② Neutron TOF spectra were preferred over gamma due to lower background and higher accuracy.

Response matrix

$$\begin{bmatrix} N_1 \\ N_2 \\ N_3 \\ \vdots \\ N_i \end{bmatrix} = \begin{bmatrix} R_{11} & R_{12} & R_{13} & \cdots & R_{1j} \\ R_{21} & R_{22} & R_{23} & \cdots & R_{2j} \\ R_{31} & R_{32} & R_{33} & \cdots & R_{3j} \\ \vdots & \vdots & \vdots & \ddots & \vdots \\ R_{i1} & R_{i2} & R_{i3} & \cdots & R_{ij} \end{bmatrix} \bullet \begin{bmatrix} \phi_1 \\ \phi_2 \\ \phi_3 \\ \vdots \\ \phi_j \end{bmatrix}$$

Neutron TOF Pulse time distribution

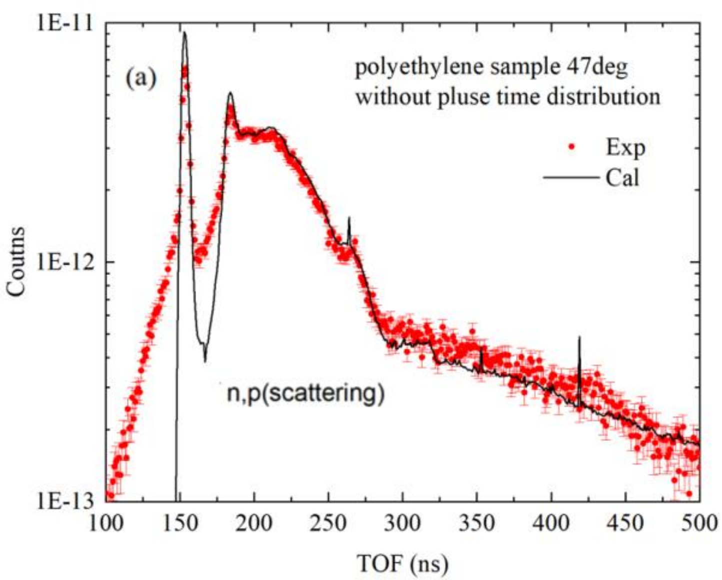

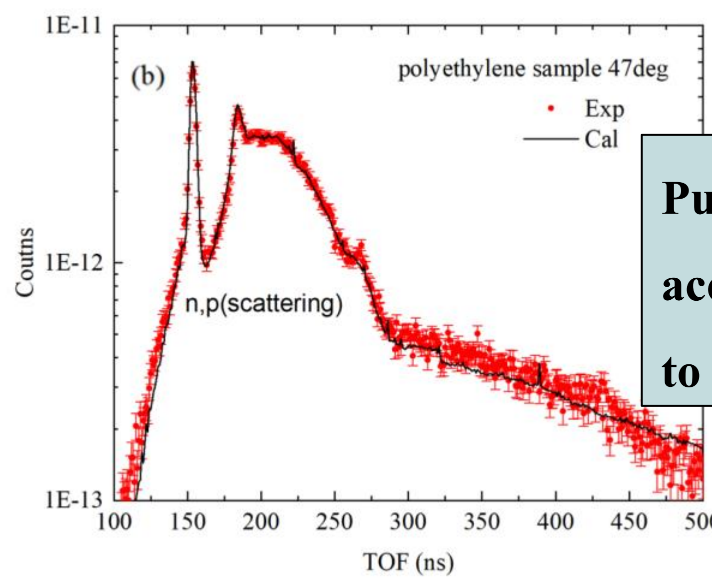

Pulse time profile accuracy is critical to result reliability.

③ Associated Particle Detection with SiC Detector

D-D neutrons inevitably accompany D-T sources due to deuteron beam deposition in the target.

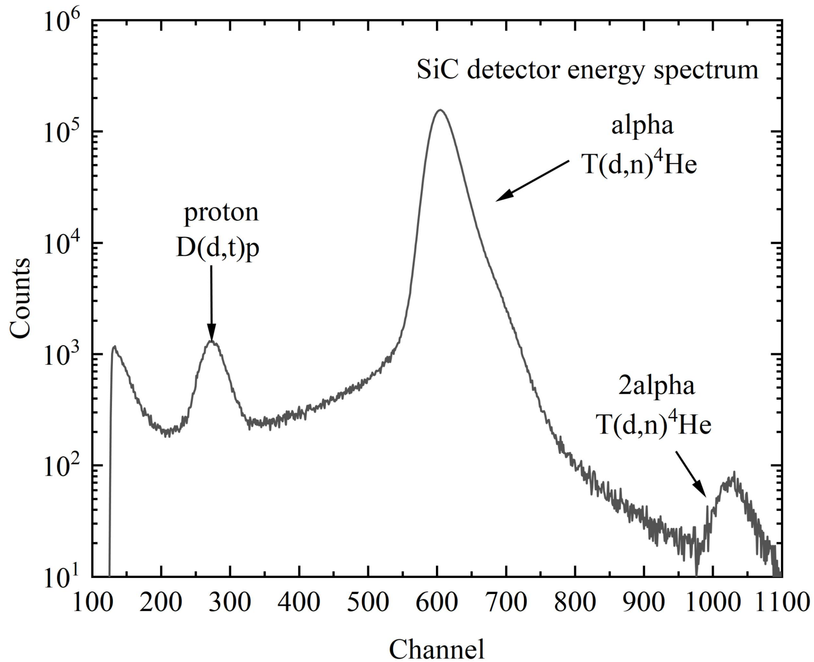

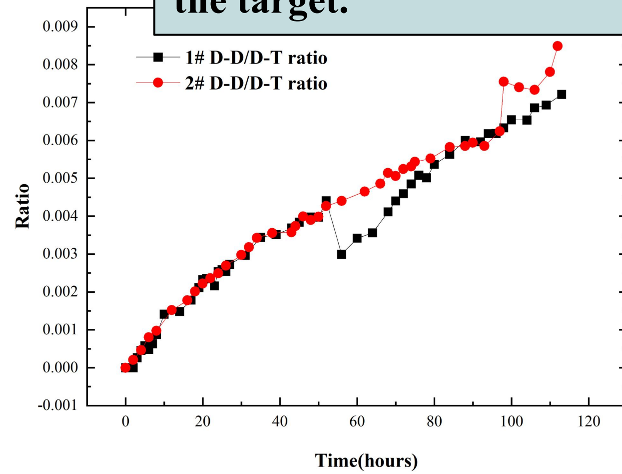

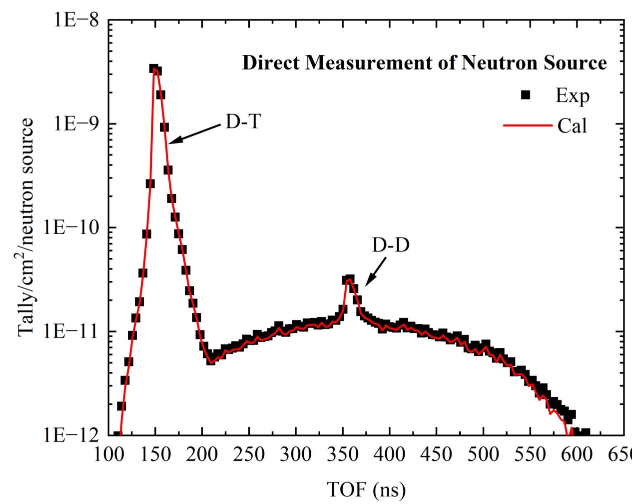

① SiC detector distinguishes DD-protons and DT-alphas;

② Enables accurate assessment of DD/DT neutron field composition.

Experimental Results – Standard Sample (CH_2)

2 Angles + 2 Conditions

①verify the accuracy and repeatability of the system.

② the n–p scattering cross section is internationally recognized.

③**Systematic uncertainty < 3%.**

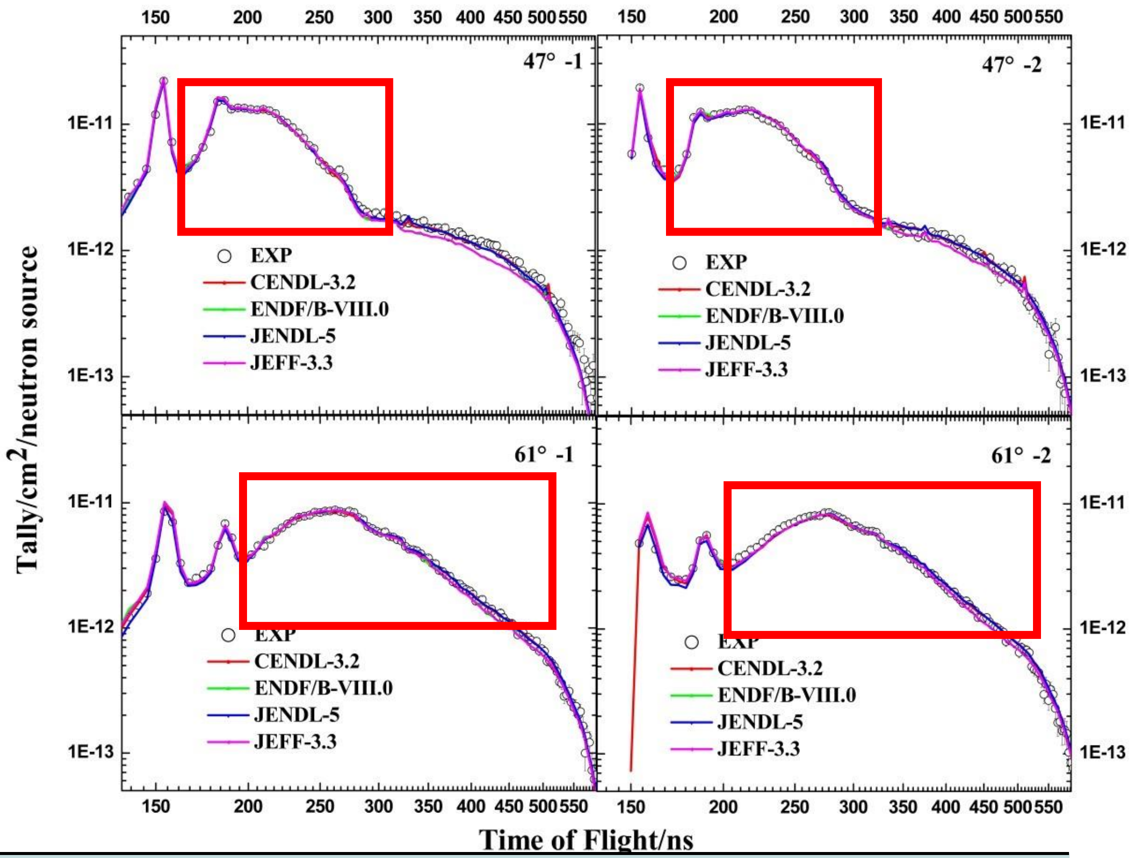

Angle	C/E value		
	CENDL-3.2	ENDF/B-VIII.0	JEDNL-5.0	JEFF-3.3
47deg-1	0.9811 ± 0.0298	0.9884 ± 0.0300	0.9738 ± 0.0296	0.9902 ± 0.0301
47deg-2	1.0013 ± 0.0304	1.0110 ± 0.0307	1.0057 ± 0.0306	1.0131 ± 0.0308
61deg-1	0.9882 ± 0.0299	0.9695 ± 0.0293	0.9961 ± 0.0301	0.9677 ± 0.0292
61deg-2	0.9931 ± 0.0301	0.9942 ± 0.0301	1.0046 ± 0.0304	0.9946 ± 0.0301

Experimental Results – Be Sample

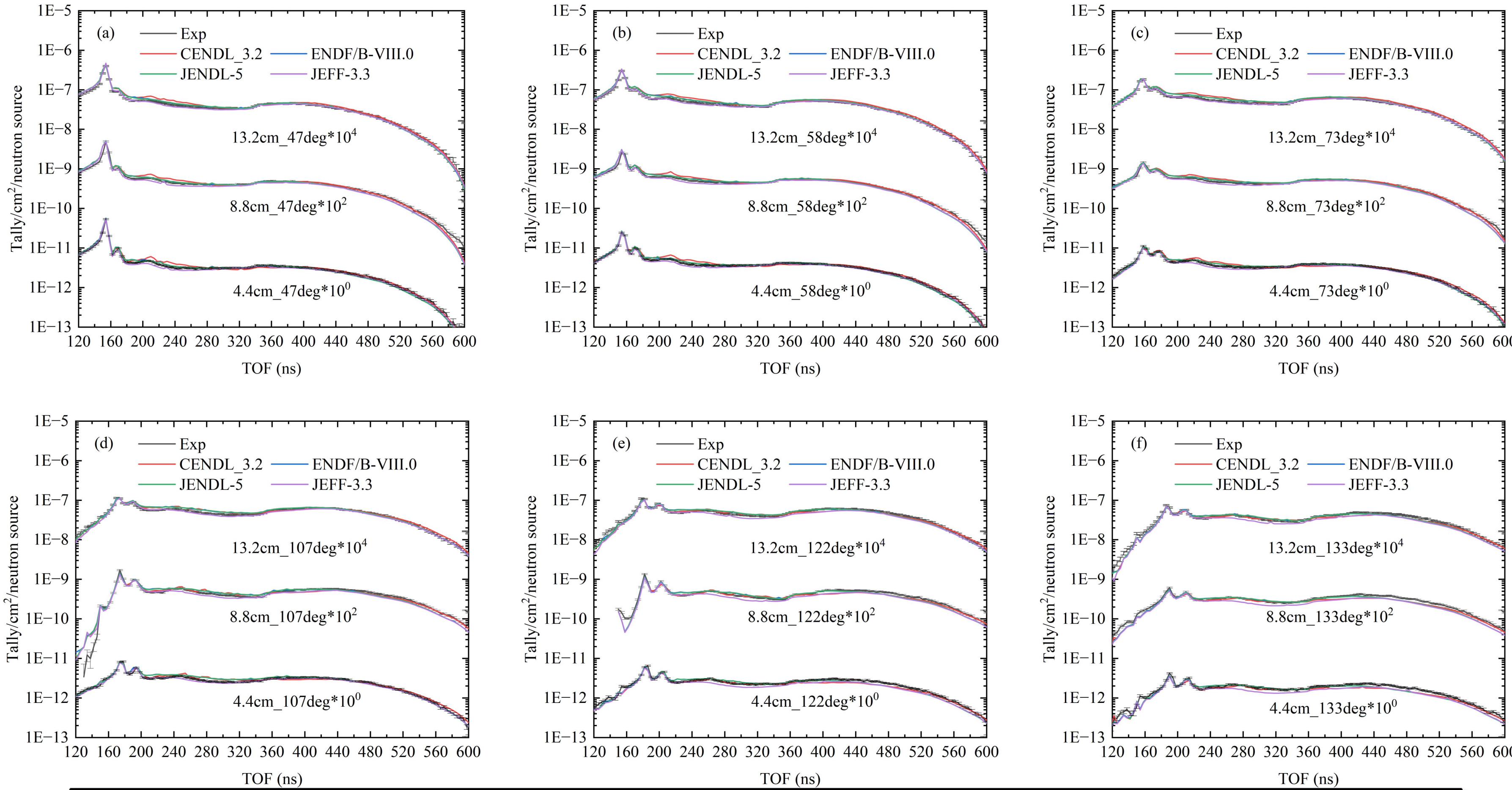

Comparison of Experimental Results with Four Nuclear Data Libraries Across Three Thicknesses and Six Scattering Angles

Experimental Results – Zr Sample

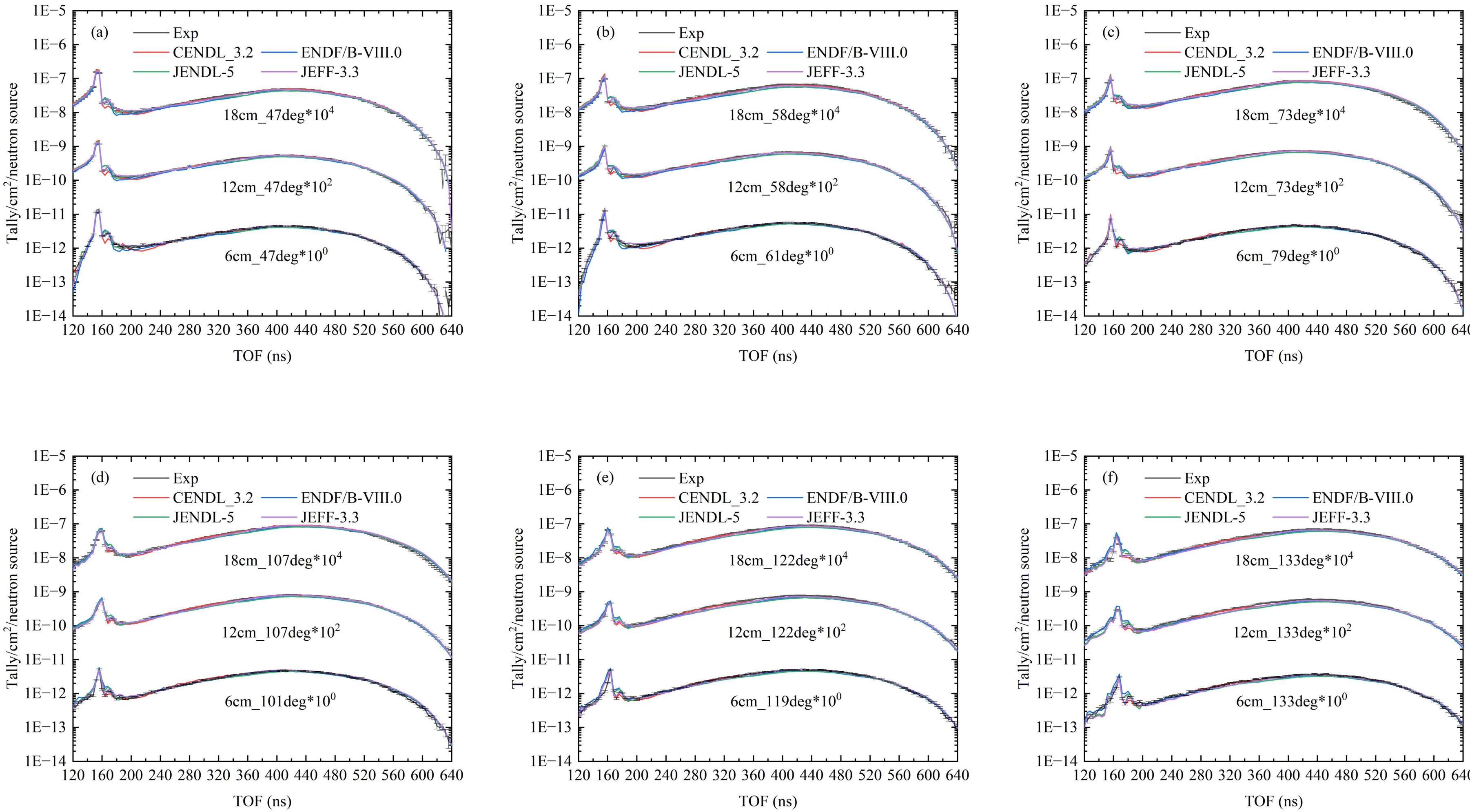

Experimental Results – Bi Sample

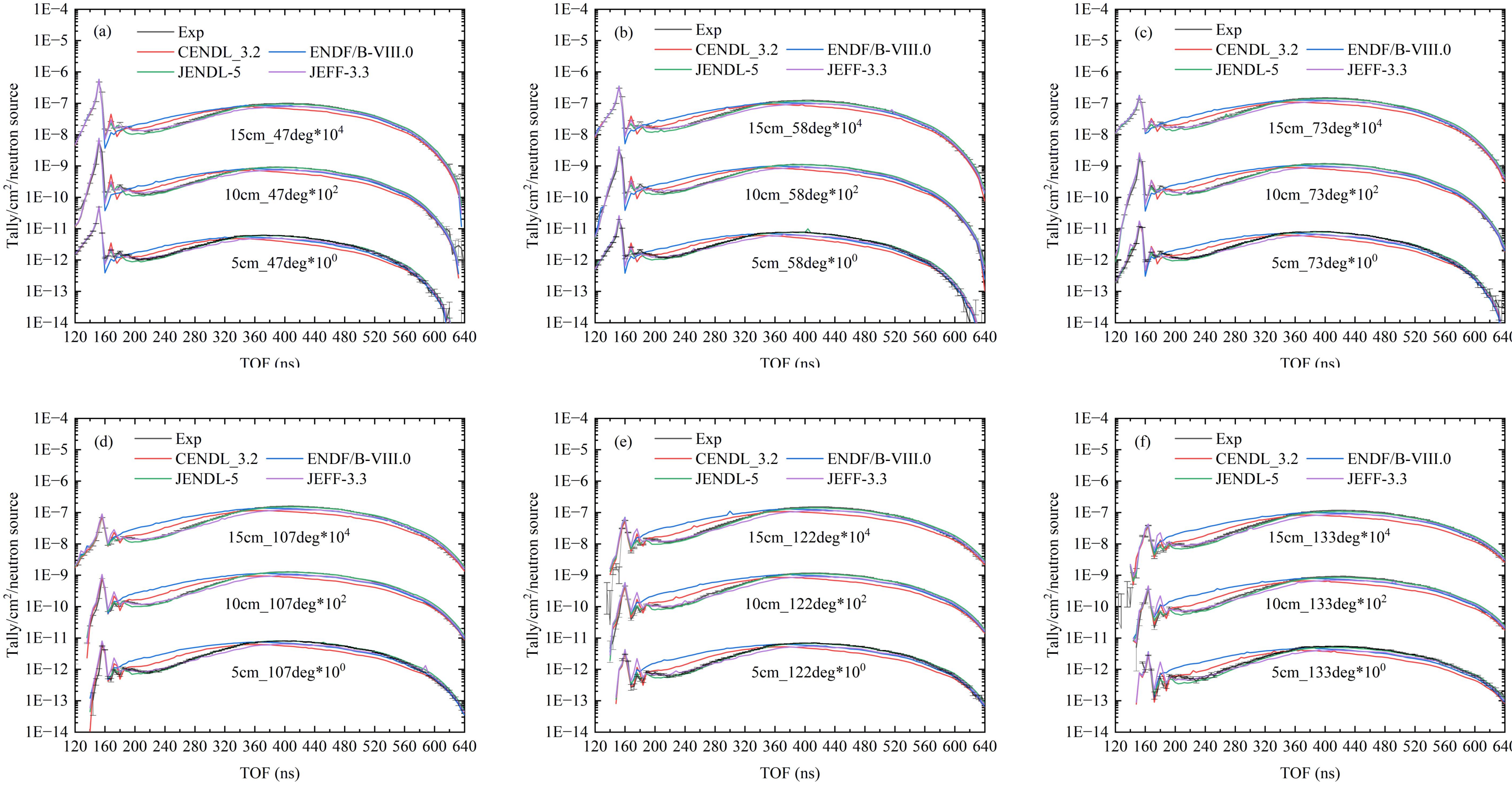

Reaction Channel Separation in TOF Spectra

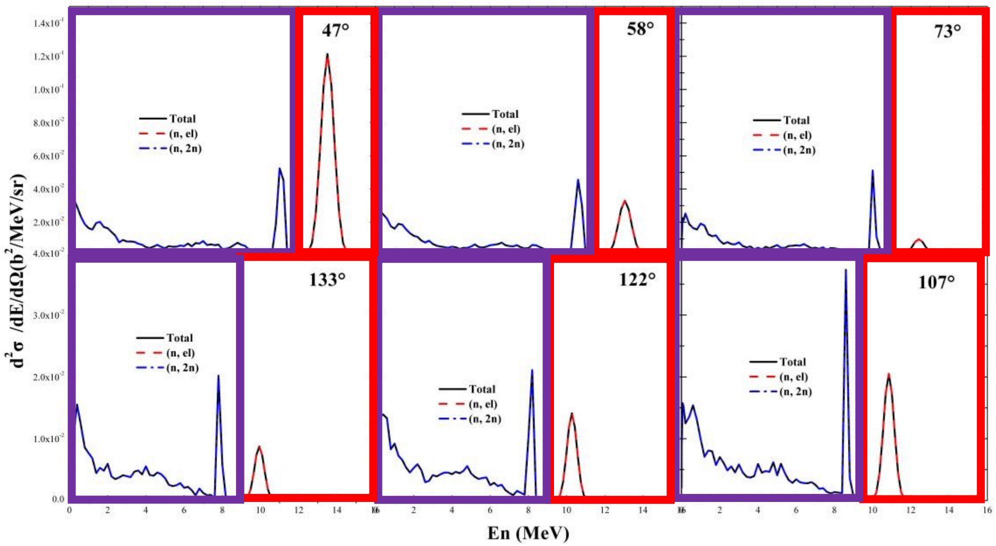

(n,2n) (n,el)

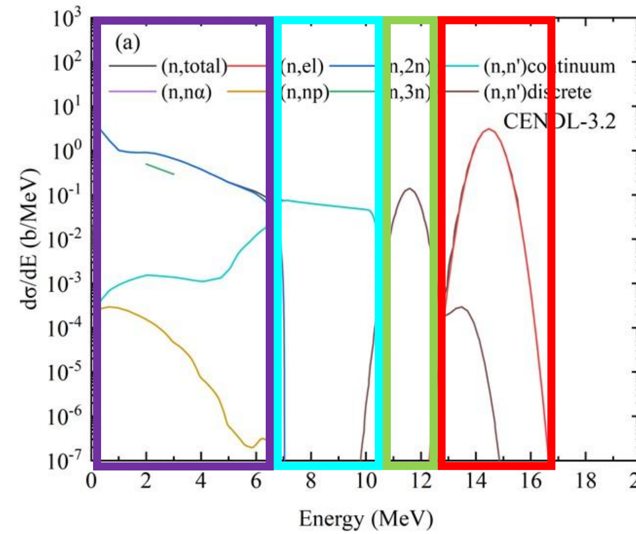

(n,2n) (n,inl)C

(n,inl)D (n,el)

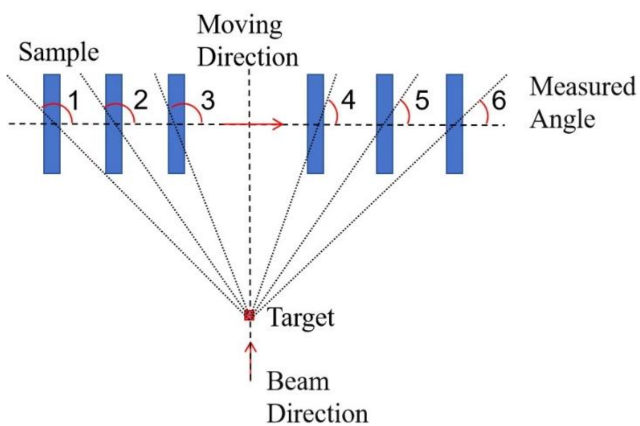

①Energy regions are defined by the dominant contribution within that range.;

②TOF windows are determined by combining flight distance and energy intervals.

Be Experimental Results Analysis (CENDL-3.2)

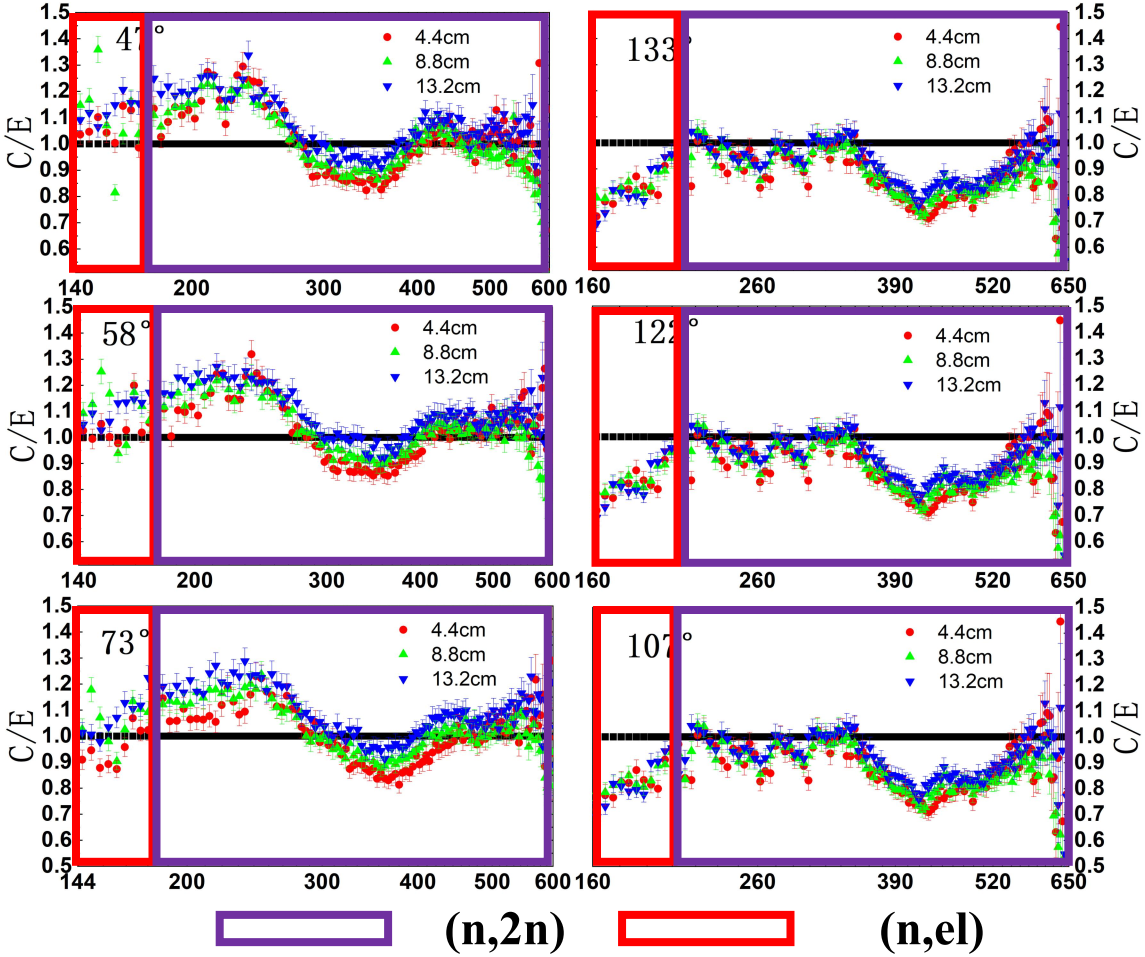

①In the elastic scattering region, CENDL-3.2 overestimates the yields at 47° and 58°, while underestimating at 107°, 122°, and 133°;

②In the (n,2n) region, CENDL-3.2 shows an overestimation at small angles in the high-energy part, and an overestimation at small angles but underestimation at large angles in the low-energy part.

Good consistency observed across different thicknesses at the same angle.

Analysis of Evaluated Data for Be

(n,2n) Reaction Cross Sections

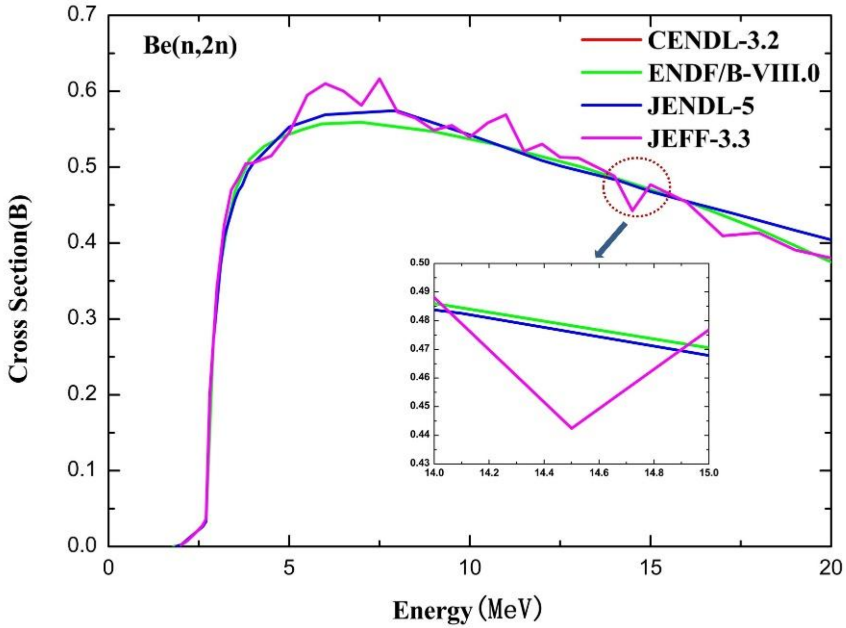

Elastic Scattering Angular Distribution of 14.5 MeV Neutrons on ^{9}Be

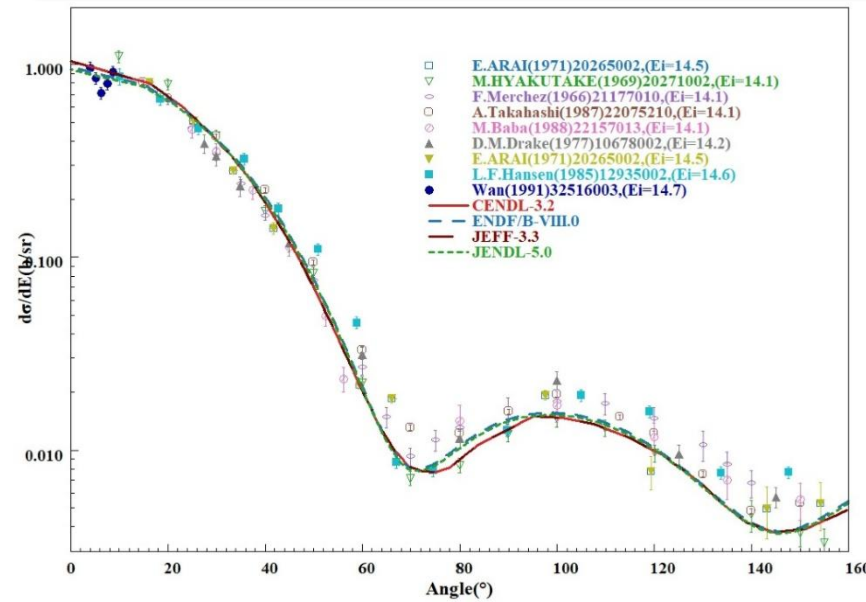

①JEFF-3.3 is notably low in the (n,2n) region.

②All libraries underestimate low-energy, large-angle results.

①Small differences among libraries;

②overestimated at small angles, underestimated at large angles.

Zr Experimental Results Analysis (CENDL-3.2)

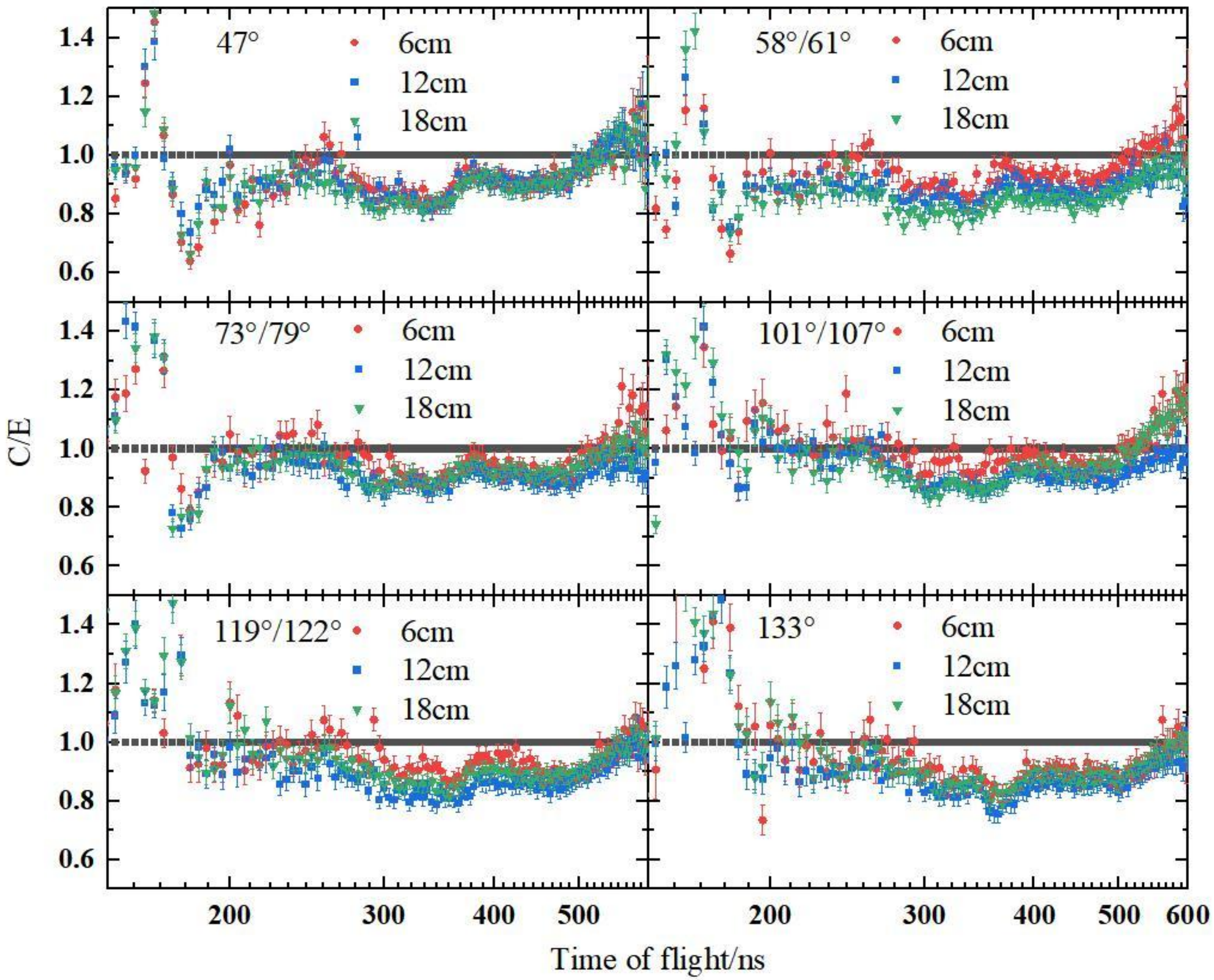

- **13.4-16 MeV, (n,el)**

C/E values increase with angle.
Lower at small angles;
higher at large angles.

- **10.6-13.4MeV, (n,inl)D**

C/E values are mostly above 1 and remain consistent across angles, with a slight rise from 122° onward.

- **4.0-10.6 MeV, (n,inl)C**

C/E values slightly increase with angle.
Shows stable angular behavior.

- **0.8-4.0 MeV, (n,2n)**

C/E values are stable with angle.
Overall magnitude is relatively low.

Analysis of Evaluated Data for Zr

Angular Distribution of 14.5 MeV Neutrons on Zr

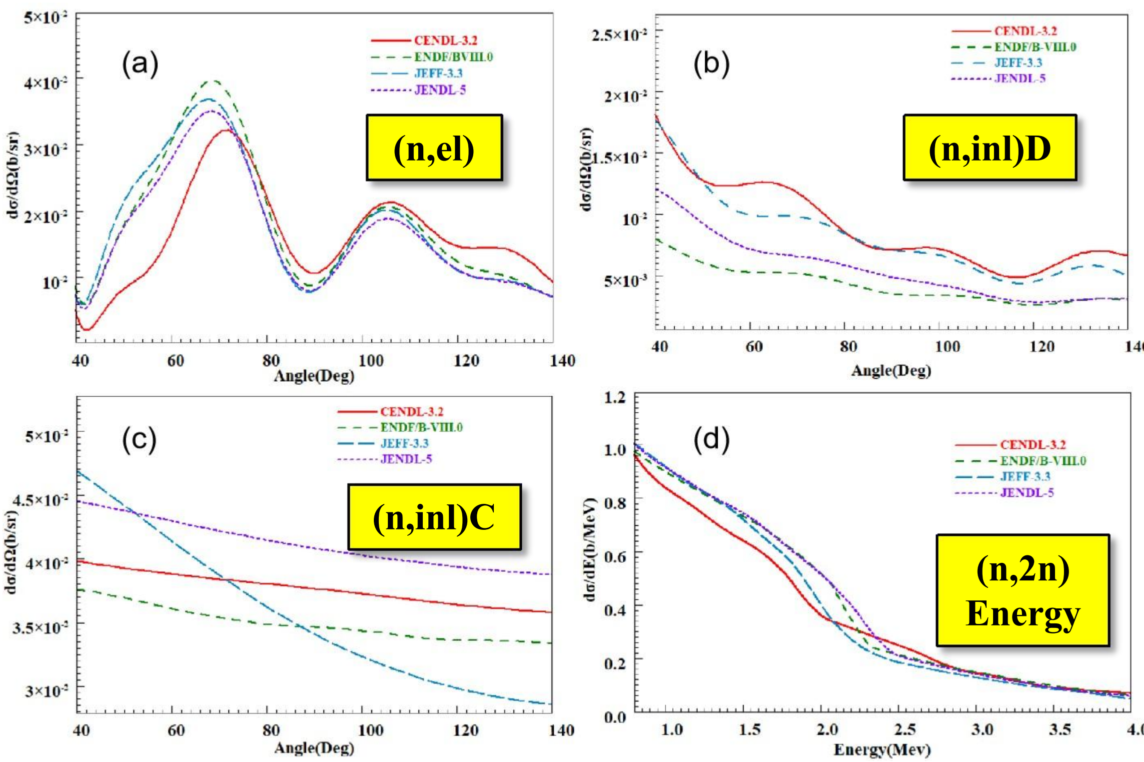

- **Elastic Region**

CENDL-3.2 performs best at small angles, while the other libraries overestimate.
At large angles, all libraries tend to overestimate.

- **Discrete-Level Inelastic Region**

Significant differences exist. ENDF/B-VIII.0 tends to underestimate, while the others generally overestimate across most angles.

- **Continuous-Level Inelastic Region**

Trends vary: some libraries show increasing C/E with angle, others decreasing. Largest discrepancies appear at backward angles.

- **(n,2n) Region:**

All libraries tend to underestimate experimental results. CENDL-3.2 and JEFF-3.3 shows the most notable underprediction.

Bi Experimental Results Analysis (CENDL-3.2)

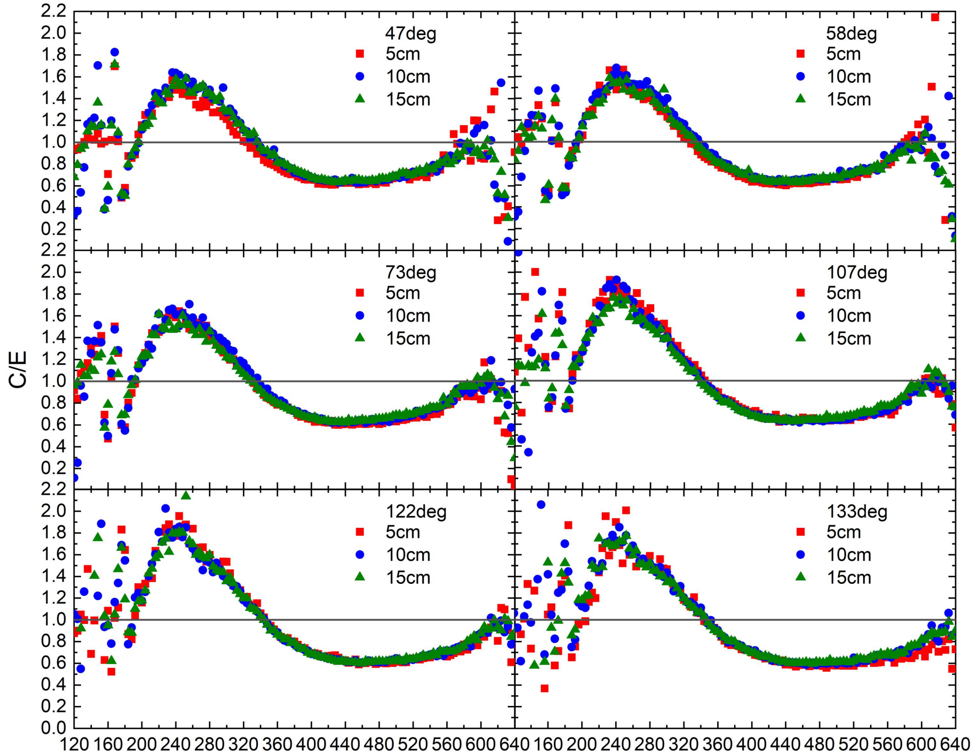

Angle (deg)	TOF (ns)			
	(n,el)	(n,n')discrete	(n,n')continuum	(n,2n)
47	132~156	160~172	176~216	220~608
58	132~160	160~172	176~216	220~616
73	132~160	164~176	180~220	224~624
107	140~160	164~176	180~224	228~636
122	144~164	168~180	184~228	232~644
133	148~168	172~184	188~232	236~652

- **Elastic Region**

C/E values increase with angle; best performance at 133°, with minimal overlap from inelastic scattering.

- **Discrete-Level Inelastic Region**

Consistently overestimates across all angles but maintains a reasonable angular trend.

- **Continuous-Level Inelastic Region**

Accurate at small angles (47°, 58°), slightly overestimates at 73°, and more significantly at large angles.

- **(n,2n) Region:**

Systematically underestimates across the entire energy range.

Analysis of Evaluated Data for Bi

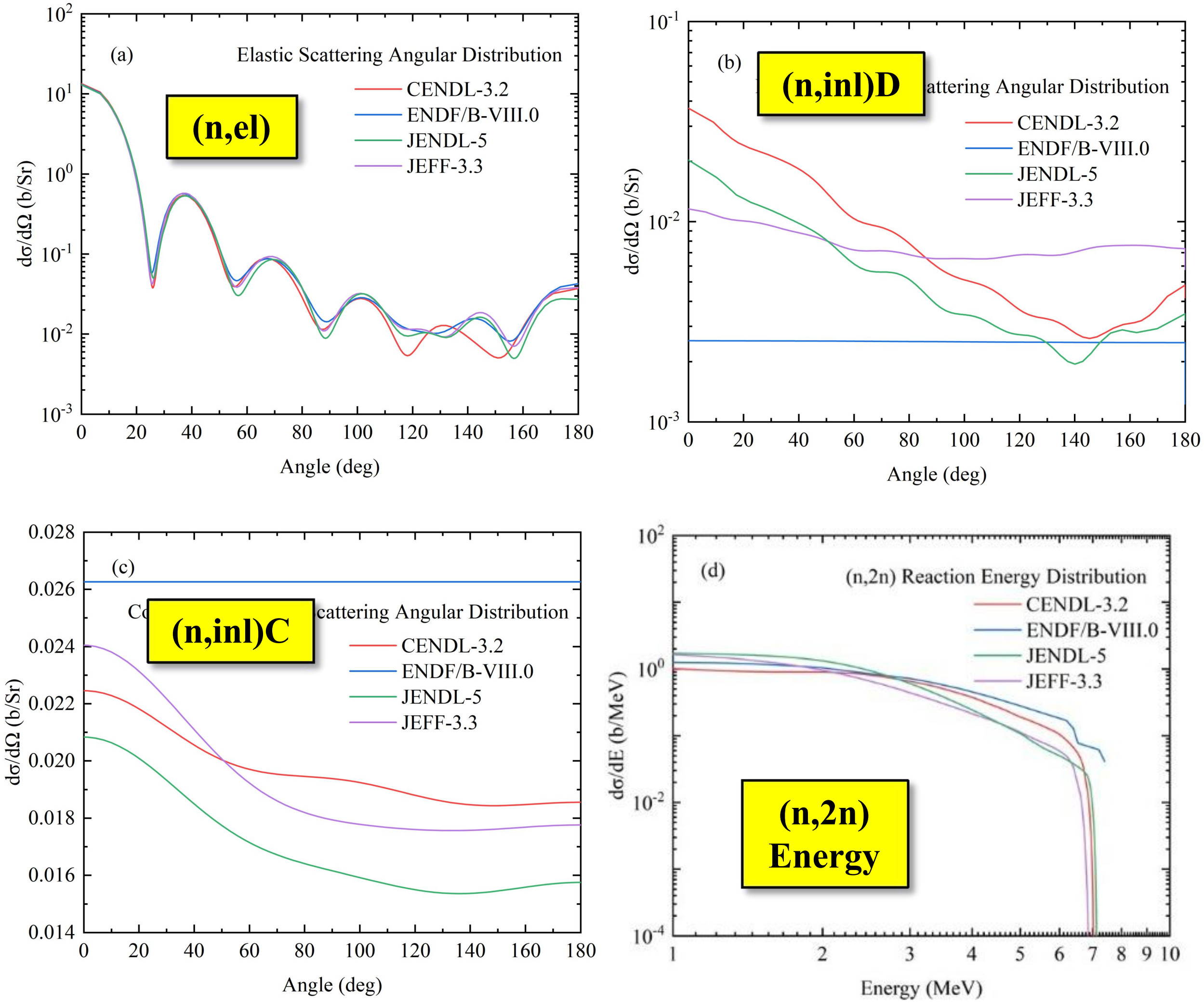

- **Elastic Region**

CENDL-3.2 provides best agreement across angles.

- **Discrete-Level Inelastic**

JENDL-5 is best at large angles; JEFF-3.3 performs well at small angles.

- **Continuous-Level Inelastic**

JEFF-3.3 is most accurate overall; CENDL-3.2 performs well at 58° .

- **(n,2n) Region:**

ENDF/B-VIII.0 shows best C/E match; JENDL-5 is more consistent across the full range.

Summary

1. Upgrades to the experimental platform significantly enhanced measurement accuracy and reliability.
2. In this work, the validation of the evaluated nuclear data for **Be/Zr/Bi** was performed.
3. The theoretical calculation was carried out by MCNP code using the evaluated nuclear data of the **CENDL-3.2, ENDF/B-VIII.0, JENDL-5 and JEFF-3.3** libraries. From the comparison, some discrepancies in different energy ranges are found.
4. In conclusion, the evaluated data of four libraries need to be improved as required in different energy ranges.

Thank you for your attention !

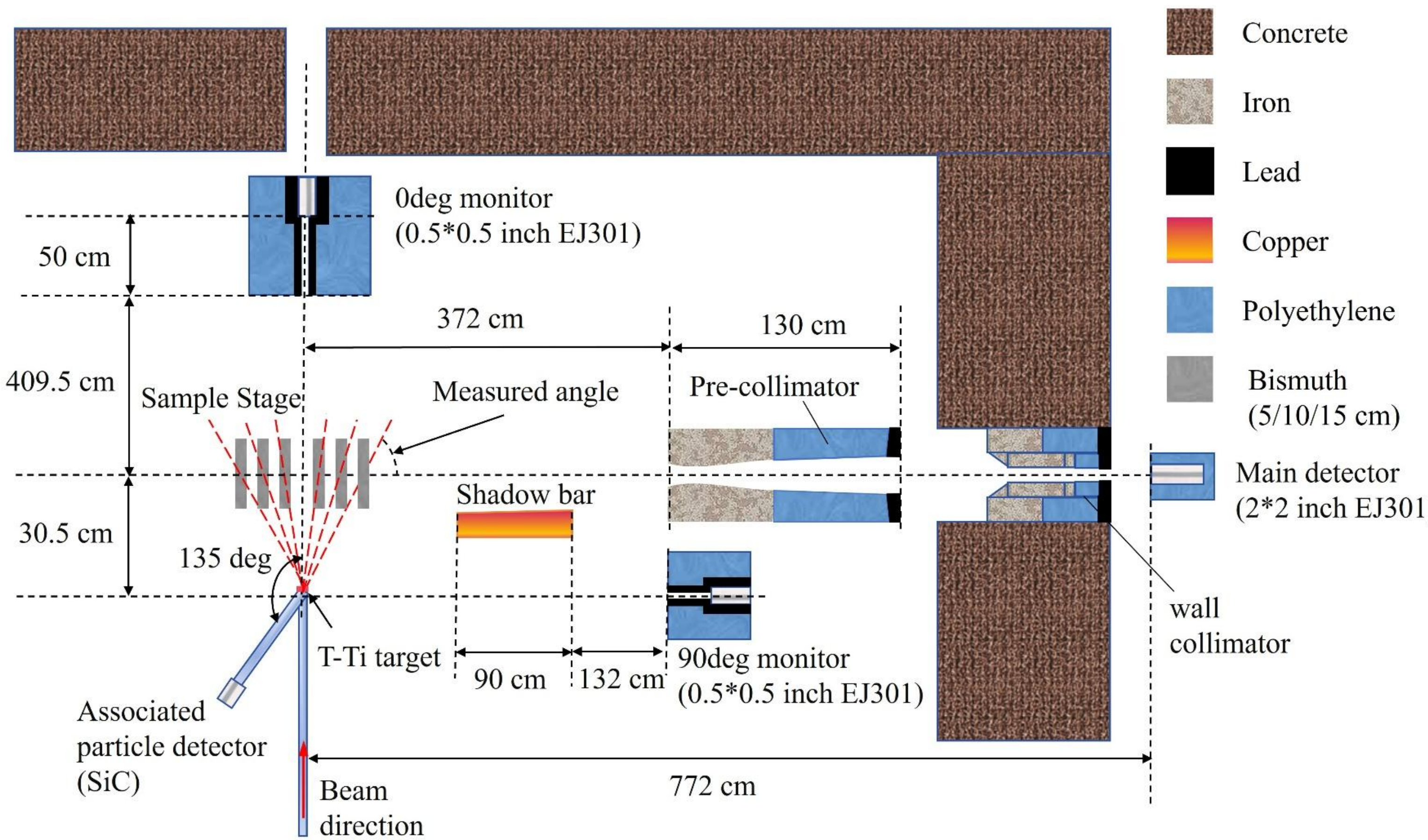

Concrete
Iron
Lead
Copper
Polyethylene
Bismuth
(5/10/15 cm)
0deg monitor
(0.5*0.5 inch EJ301)
50 cm
372 cm
130 cm
409.5 cm
Sample Stage
Measured angle
Pre-collimator
Main detector
(2*2 inch EJ301)
Shadow bar
30.5 cm
135 deg
T-Ti target
90 cm
132 cm
90deg monitor
(0.5*0.5 inch EJ301)
wall
collimator
Associated
particle detector
(SiC)
Beam
direction
772 cm

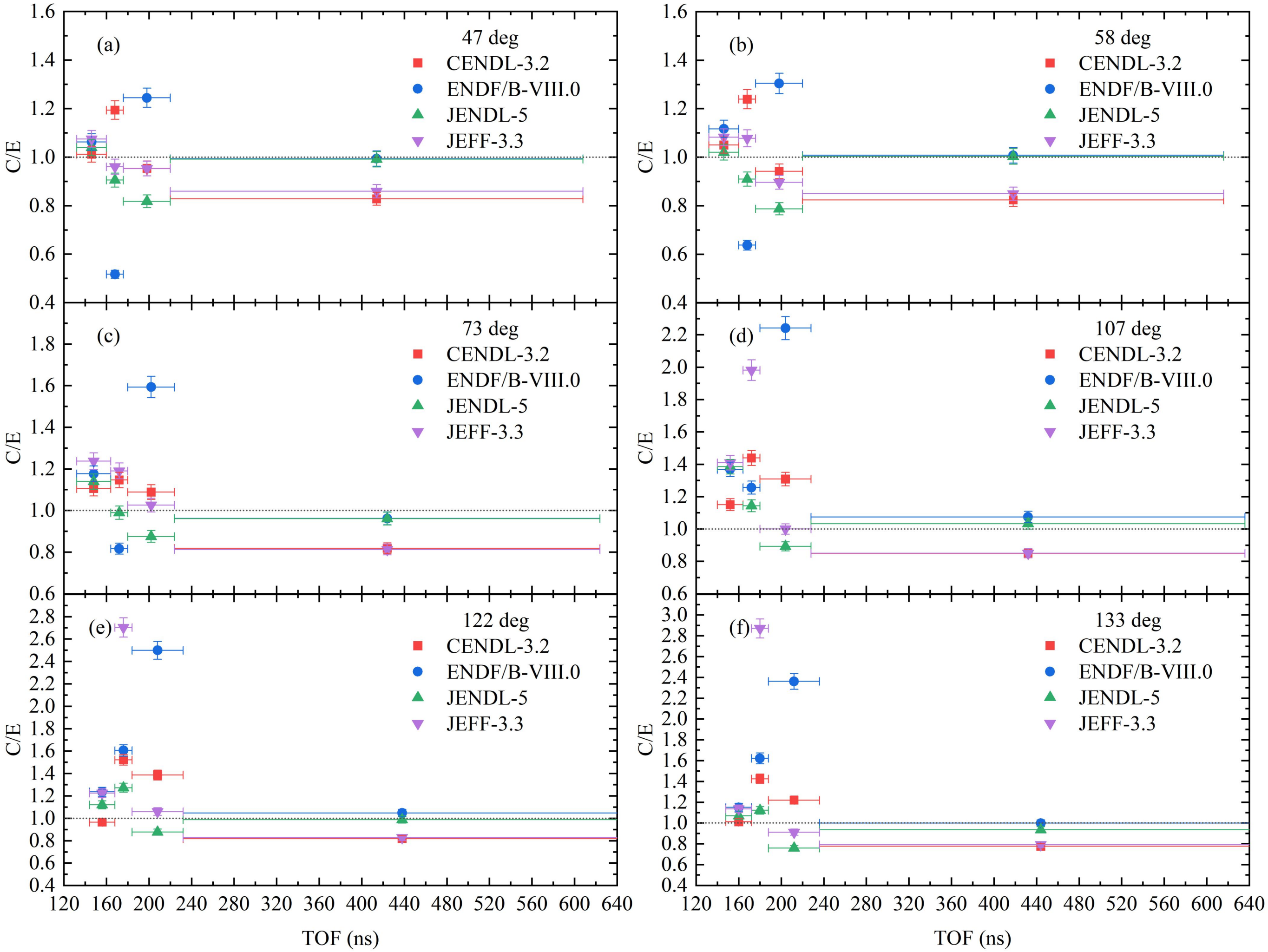

(a)
47 deg
(b)
58 deg
(c)
73 deg
(d)
107 deg
(e)
122 deg
(f)
133 deg
CENDL-3.2
ENDF/B-VIII.0
JENDL-5
JEFF-3.3
C/E
TOF (ns)

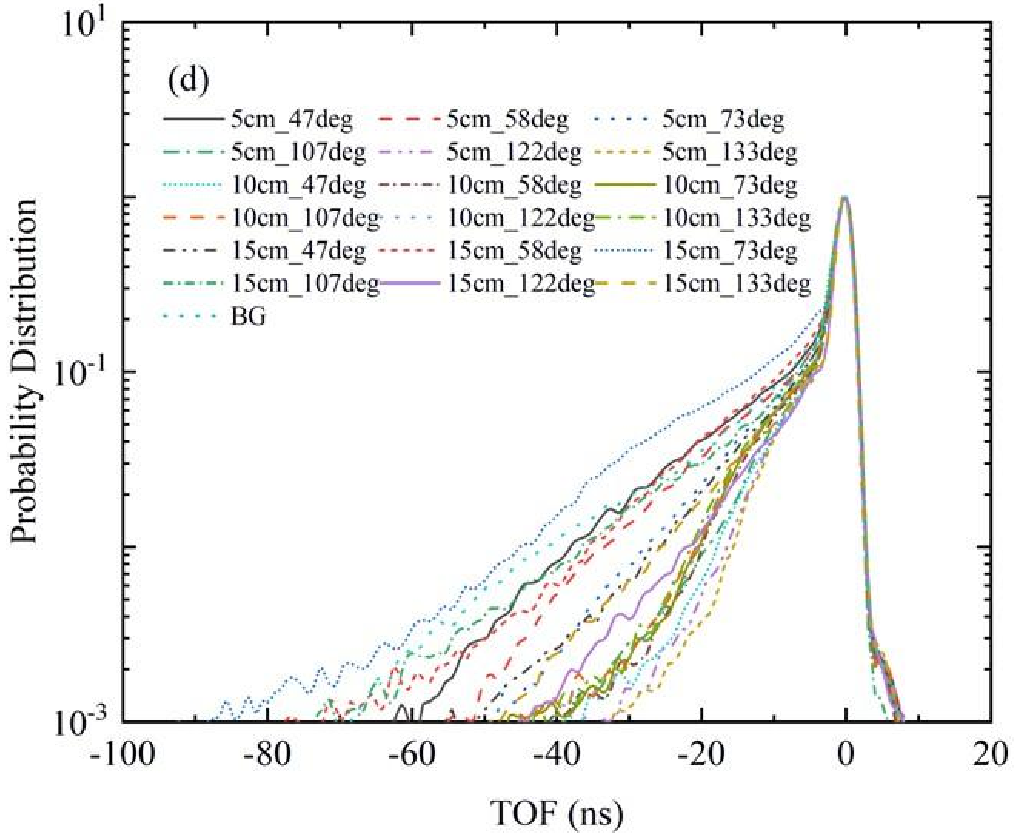
(d)
5cm_47deg
5cm_58deg
5cm_73deg
5cm_107deg
5cm_122deg
5cm_133deg
10cm_47deg
10cm_58deg
10cm_73deg
10cm_107deg
10cm_122deg
10cm_133deg
15cm_47deg
15cm_58deg
15cm_73deg
15cm_107deg
15cm_122deg
15cm_133deg
BG
Probability Distribution
TOF (ns)
10^1
10^{-1}
10^{-3}
-100
-80
-60
-40
-20
0
20

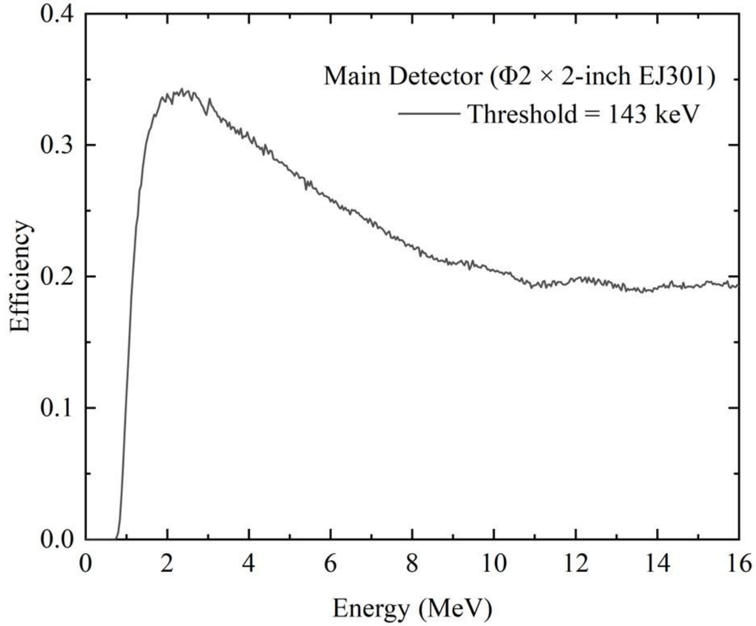
Main Detector (Φ2 × 2-inch EJ301)
Threshold = 143 keV
Efficiency
Energy (MeV)
0.0
0.1
0.2
0.3
0.4
0
2
4
6
8
10
12
14
16

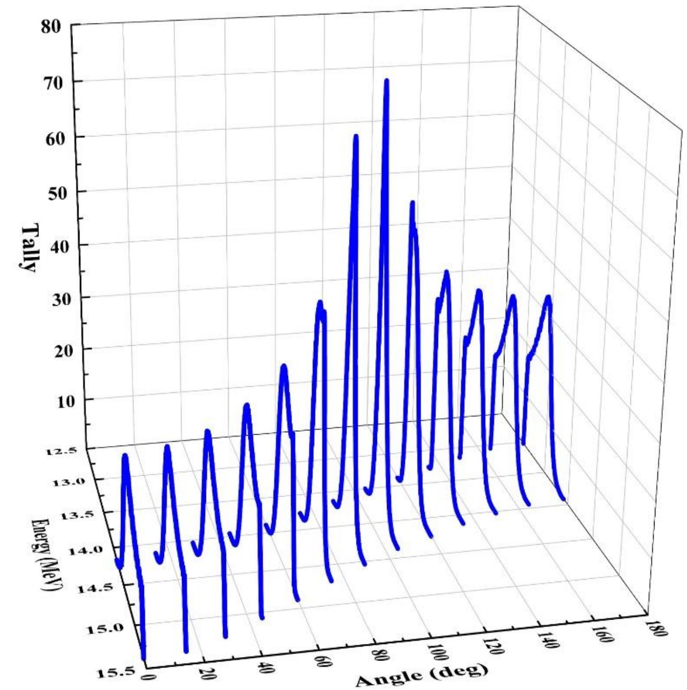
Tally
Energy (MeV)
Angle (deg)
10
20
30
40
50
60
70
80
12.5
13.0
13.5
14.0
14.5
15.0
15.5
0
20
40
60
80
100
120
140
160
180

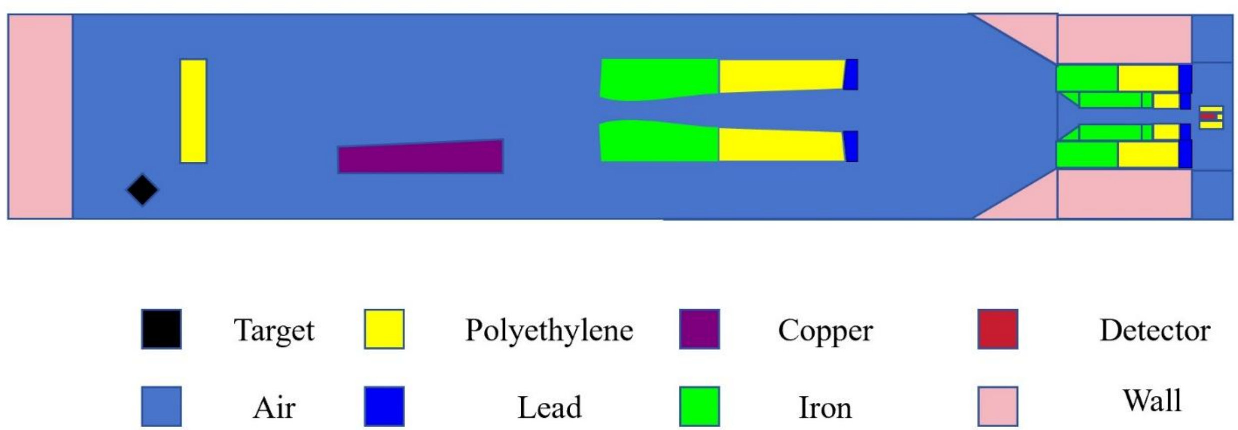
Target
Polyethylene
Copper
Detector
Air
Lead
Iron
Wall